AIMS Mathematics, 11(4): 9587–9611.
DOI: 10.3934/math.2026397
Received: 03 December 2025
Revised: 26 February 2026
Accepted: 03 March 2026
Published: 10 April 2026

http://www.aimspress.com/journal/Math

Research article

Dynamics, bifurcation, and chaos control in a fractional-order discrete multi-team predator–prey model

Mahmoud A. M. Abdelaziz[1,2], Elhadi E. Elamir[1,2,*], Ibrahim M. E. Abdelsatar[3], A. A. Al Qarni[4], Manal Alqhtani[1,2], Montaser O. S. Hilal[3] and A. A. Elsadany[5]

[1] Department of Mathematics, Faculty of Science and Arts, Najran University, Najran 66445, Saudi Arabia

[2] Science and Engineering Research Center, Najran University, Najran, Saudi Arabia

[3] Department of Management Information Systems, College of Business and Economics, Qassim University, Buraidah 51452, Saudi Arabia

[4] Department of Mathematics, College of Science, University of Bisha, P.O. Box 551, Bisha 61922, Saudi Arabia

[5] Department of Mathematics, College of Sciences and Humanities, Prince Sattam Bin Abdulaziz University, Al-Kharj 11942, Saudi Arabia

* **Correspondence:** Email: aialamer@nu.edu.sa; Tel: +966506087979.

Abstract: In this paper, a discrete-time fractional-order multi-team predator–prey model derived from a Caputo-type fractional framework was proposed and analyzed. The model describes the nonlinear interactions between two cooperating prey populations and a common predator species, where the fractional-order parameter modulates the influence of past states through the fractional discrete formulation. An algebraic stability criterion based on the characteristic polynomial coefficients of the Jacobian matrix was employed to investigate the local asymptotic stability of the coexistence equilibrium without relying on explicit eigenvalue computations. The necessary and sufficient analytical conditions for the occurrence of flip and Neimark–Sacker (NS) bifurcations were derived, and the associated codimension-two flip–NS bifurcation was rigorously characterized. Numerical simulations validated the theoretical results and revealed complex dynamical behaviors, including periodic oscillations, quasiperiodicity, and chaos. To suppress unstable oscillations, three chaos control strategies—Ott–Grebogi–Yorke (OGY) feedback control, hybrid control, and state feedback control—were implemented. A systematic quantitative comparison based on convergence speed, control effort, and stabilization robustness was conducted to evaluate their relative performance and to clarify their ecological management implications. The results showed that the fractional-order parameter significantly affects stability thresholds and bifurcation organization, thereby reshaping the qualitative structure of population dynamics. These findings highlight the regulatory role of fractional-order effects in discrete ecological systems and provide a rigorous framework for stability analysis and

controlled ecosystem management.

Keywords: mathematical model; fractional difference equations; predator–prey model; algebraic stability criterion; flip bifurcation; Neimark–Sacker bifurcation; codimension-two bifurcation; discrete dynamical systems; chaos control
Mathematics Subject Classification: 39A30, 37G15

1. Introduction

Mathematical modeling provides a powerful and cost-effective framework for investigating biological systems, offering an alternative to resource-intensive field and laboratory experiments. Such models complement empirical studies by facilitating efficient data utilization and enabling researchers to gain deeper insight into mechanisms that are often difficult to observe directly. Through systematic abstraction, mathematical models preserve the essential characteristics of complex biological systems and frequently reveal rich dynamical behaviors such as bifurcation and chaos [1].

Bifurcation theory examines how the qualitative behavior of a dynamical system changes when a governing parameter is varied. The concept, first introduced by Henri Poincaré, has evolved into a fundamental analytical tool for identifying and interpreting transitions between distinct dynamical regimes [2]. Continuous developments in bifurcation theory have strengthened its connections with various branches of science and engineering, allowing researchers to anticipate and classify stability changes in complex systems [3].

In ecological modeling, bifurcation analysis has been widely applied to investigate interactions among multiple species. These models frequently incorporate ecological mechanisms such as crowding, age structure, time delay, and nonlinear functional responses [4]. In many ecosystems, cooperation and spatial proximity among individuals enhance foraging efficiency and reduce predation risk. Understanding such cooperative and competitive behaviors is therefore essential for constructing realistic predator–prey models [5].

Classical predator–prey systems involving two prey species and a single predator often exhibit instability, in which the predator ultimately dominates. Simply analyzing attack rates as a function of prey density is insufficient to capture the adaptive strategies that species use to evade predation. Recent research has shown that simplified models can nevertheless reproduce the essential features of real ecological systems. Depending on parameter values, such systems may exhibit extinction, coexistence, or oscillatory behavior [6]. For instance, stochastic logistic-type formulations have revealed unexpected long-term outcomes in threatened populations, while other studies indicate that the persistence of non-trivial dynamics may require high dispersal rates, interspecific competition, or contrasting growth and decay timescales between species [7].

A notable contribution to cooperative predator–prey modeling was presented by Elettreby [8], who introduced a multi-team ecological framework describing the interaction between two cooperating prey populations and a common predator. This foundational model has since inspired several extensions incorporating time delays, memory effects, and additional ecological mechanisms, highlighting the importance of cooperation in prey defense and predator regulation. In the present work, this

cooperative framework is adopted as a baseline for constructing a discrete-time fractional-order model with memory [9, 10].

In recent years, several studies have investigated integer-order and fractional-order predator–prey models in both continuous and discrete settings, reflecting the increasing interest in memory-dependent ecological dynamics [11, 12]. For example, fractional predator–prey systems with time delay and harvesting have been analyzed to reveal complex bifurcation structures and long-term memory effects, while discrete fractional models have shown that memory can significantly modify stability regions and transition routes to chaos [13]. Compared with these existing works, the present study differs in three essential aspects: (i) it considers a cooperative multi-team interaction mechanism between two prey populations and a common predator, (ii) it adopts a discrete-time fractional framework to simultaneously capture memory and sampling effects, and (iii) it provides a complete analytical characterization of flip, Neimark–Sacker (NS), and codimension-two flip–NS bifurcations using algebraic stability criteria. These features allow the proposed model to offer new qualitative insight into how fractional memory reshapes the dynamical organization of cooperative ecological systems.

During the past three decades, fractional calculus has emerged as an essential mathematical tool for describing memory-dependent and hereditary processes in biological systems [12]. Unlike classical integer-order models, fractional-order systems are non-local, with their future behavior determined by both current and historical states [9]. This inherent memory effect can significantly influence dynamical behavior, making fractional-order formulations particularly suitable for complex biological interactions [14].

In this study, Caputo's definition of the fractional derivative is adopted because it incorporates standard initial and boundary conditions and aligns well with experimentally observed biological phenomena. Fractional-order modeling is especially relevant for predator–prey systems, where memory effects arise from adaptive learning, delayed responses, and cumulative ecological interactions [15].

Motivated by earlier studies on cooperative predator–prey interactions, this work introduces a discrete-time formulation of a multi-team predator–prey model with fractional-order memory. The discrete fractional framework allows a systematic investigation of stability variations and bifurcation patterns arising from the combined effects of temporal discretization and memory-dependent dynamics. The paper is organized as follows. Section 2 presents the mathematical formulation of the discrete-time fractional-order model. Section 3 addresses the existence and uniqueness of solutions. Section 4 is devoted to the local stability analysis of the equilibrium points. Bifurcation phenomena, including flip, NS, and flip–NS bifurcations, are investigated in Section 5. Numerical simulations are provided in Section 6 to support the theoretical results, while Section 7 concludes the paper and outlines possible directions for future research.

Although predator–prey systems, fractional-order models, and discrete-time dynamics have each been widely investigated in the literature, their combined interaction in a cooperative multi-team ecological framework remains largely unexplored. The main novelties and contributions of this work can be summarized as follows. First, a discrete-time fractional-order multi-team predator–prey model with cooperative prey defense is proposed, extending classical continuous multi-prey predator formulations to a memory-dependent discrete setting. Second, unlike most existing studies that rely on direct eigenvalue computation, an algebraic stability criterion based on the characteristic polynomial coefficients is employed to investigate local stability and bifurcation behavior. Third, the necessary and

sufficient analytical conditions for NS, flip, and codimension-two flip–NS bifurcations are explicitly derived for the proposed fractional discrete model, which, to the best of our knowledge, has not been previously reported for such ecological systems. Fourth, the 0–1 test for chaos is applied to rigorously distinguish regular from chaotic dynamics in the fractional discrete framework. Finally, three different chaos control strategies—Ott–Grebogi–Yorke (OGY) feedback control, hybrid control, and state feedback control—are implemented and comparatively analyzed for stabilizing chaotic dynamics. These results demonstrate that fractional-order memory significantly enriches nonlinear behavior and provides additional mechanisms for controlling instability in discrete ecological systems.

2. Model formulation: a continuous, fractional, and discrete-time framework

In this section, we first recall the baseline continuous-time cooperative predator–prey model that forms the foundation of our study. This classical formulation is then extended to a fractional-order framework in order to incorporate memory effects. Finally, a discrete-time fractional map is derived using an appropriate discretization scheme for the subsequent stability, bifurcation, and chaos analysis.

2.1. Construction of the multi-team predator–prey model

2.1.1. Continuous-time model

Following the cooperative ecological framework proposed by Elettreby [8], we consider a continuous-time predator–prey system describing the interaction between two cooperating prey populations and a common predator. In the absence of predation, the prey populations grow logistically, while cooperative defense mechanisms reduce predation efficiency and enhance population persistence. The model is given by

$$\begin{aligned} \frac{dL(t)}{dt} &= aL(1-L) - LN + LMN, \\ \frac{dM(t)}{dt} &= bM(1-M) - MN + LMN, \\ \frac{dN(t)}{dt} &= \beta LN + qMN - cN^2, \end{aligned} \tag{2.1}$$

where $L(t)$ and $M(t)$ represent the densities of the two cooperating prey populations, and $N(t)$ denotes the predator population. The parameters a and b denote the intrinsic growth rates of the prey, β and q represent the predator conversion efficiencies, and c measures intraspecific competition within the predator species.

2.1.2. Fractional-order model

Fractional calculus extends the classical notions of differentiation and integration to arbitrary real orders, offering a powerful mathematical framework for capturing memory-dependent and hereditary phenomena. This approach has proved highly effective in modeling a wide variety of processes arising in fields such as biology, fluid mechanics, and medical sciences [16, 17]. Several definitions of fractional differentiation exist in the literature, among which the Caputo and Riemann–Liouville (R–L) operators are the most commonly adopted [18]. The Caputo derivative is often preferred in practical applications because it allows the use of conventional initial and boundary conditions and assigns a zero derivative to constant functions, in contrast to the R–L formulation [19].

The Caputo fractional derivative of order $\alpha > 0$ of a sufficiently smooth function $x(t)$ is defined as [18, 19]

$$ {}^{C}D_t^{\alpha} x(t) = \frac{1}{\Gamma(n-\alpha)} \int_0^t \frac{x^{(n)}(\tau)}{(t-\tau)^{\alpha-n+1}}\, d\tau, \quad n-1 < \alpha < n,\ n \in \mathbb{N}. \tag{2.2} $$

In particular, for $0 < \alpha < 1$, this reduces to

$$ {}^{C}D_t^{\alpha} x(t) = \frac{1}{\Gamma(1-\alpha)} \int_0^t \frac{x'(\tau)}{(t-\tau)^{\alpha}}\, d\tau. \tag{2.3} $$

In biological systems, memory effects play a fundamental role because past ecological interactions influence present and future dynamics. These effects are particularly evident in predator–prey systems, where adaptive learning, migration, delayed reproduction, or seasonal dormancy may occur [20, 21]. Consequently, fractional-order models provide a more realistic representation of such behaviors. Caputo's derivative has therefore become a standard tool for constructing biologically meaningful fractional dynamical models [22].

Based on the continuous-time model in Eq (2.1), the corresponding fractional-order formulation can be expressed as

$$ \begin{aligned} D^{\alpha} L(t) &= aL(1-L) - LN + LMN, \\ D^{\alpha} M(t) &= bM(1-M) - MN + LMN, \\ D^{\alpha} N(t) &= \beta LN + qMN - cN^2, \end{aligned} \tag{2.4} $$

where $0 < \alpha \leq 1$, and D^{α} denotes the Caputo fractional derivative.

The conventional integer-order formulation neglects the effects of memory and delayed behavioral responses. In reality, anti-predator mechanisms and ecological adaptations evolve continuously over time. Incorporating fractional dynamics allows the model to capture such long-term memory effects, leading to richer and more realistic dynamical behavior [23, 24].

2.1.3. Discrete-time fractional model

To analyze discrete-time behavior and explore the influence of time-step size on stability and bifurcation patterns, the fractional system (2.4) is discretized using the piecewise constant argument method [25]. The resulting discrete-time fractional-order multi-team predator–prey model takes the form

$$ \begin{aligned} L_{n+1} &= L_n + \frac{h^{\alpha}}{\Gamma(\alpha+1)} \left[aL_n(1-L_n) - L_nN_n + L_nM_nN_n \right], \\ M_{n+1} &= M_n + \frac{h^{\alpha}}{\Gamma(\alpha+1)} \left[bM_n(1-M_n) - M_nN_n + L_nM_nN_n \right], \\ N_{n+1} &= N_n + \frac{h^{\alpha}}{\Gamma(\alpha+1)} \left[\beta L_nN_n + qM_nN_n - cN_n^2 \right], \end{aligned} \tag{2.5} $$

where $h > 0$ is the time-step size, and $L_n = L(n)$, $M_n = M(n)$, and $N_n = N(n)$ denote the discrete-time populations of the two prey groups and the predator, respectively, with initial conditions $L_0 > 0$, $M_0 > 0$, and $N_0 > 0$ for $n \geq 0$.

The discretization introduces an additional control parameter h, which influences both stability and dynamic transitions. As h increases, the system may undergo bifurcations leading to oscillatory or chaotic states. Thus, the discrete fractional framework captures historical ecological memory while also revealing the impact of temporal sampling on system dynamics.

2.2. Biological interpretation of parameters and fractional memory

In the proposed model, the state variables L_n, M_n, and N_n represent the population densities of the two cooperative prey groups and the predator species at the discrete time level n, respectively. The parameters a and b denote the intrinsic growth rates of the two prey populations in the absence of predation, while β and q measure the conversion efficiency of consumed prey biomass into predator reproduction. The parameter c represents the strength of intraspecific competition within the predator population, reflecting limitations in resources and territorial effects. The interaction terms LN and MN model predation pressure, whereas the cooperative defense term LMN characterizes the mutual assistance between the two prey teams in reducing predation efficiency.

The fractional order $0 < \alpha \leq 1$ plays a central role in describing memory and hereditary effects in the predator–prey interaction process. Ecologically, the memory effect may arise from repeated predator encounters, adaptive learning strategies, delayed reproductive responses, cumulative environmental influences, or persistence of past population pressure. Smaller values of α correspond to stronger memory effects, while $\alpha \to 1$ recovers the classical memory-free discrete system. Hence, the fractional parameter α provides a biologically meaningful control on the degree of historical dependence in the population dynamics [26, 27].

The discretization step size h represents the observation or reproduction time scale of the ecosystem. Variations in h correspond to changes in sampling frequency or generational time resolution, which may significantly affect stability properties and nonlinear transitions in the system.

3. Well-posedness of the fractional model and the discrete map

In this section, we establish the well-posedness of both the continuous fractional prototype and the corresponding discrete-time fractional map. Since the discrete system (2.5) is generated through a direct recursive iteration, its solution sequence is uniquely defined for all $n \geq 0$ provided that the initial conditions (L_0, M_0, N_0) are specified. Nevertheless, to ensure the physical and mathematical consistency of the fractional formulation, we first verify the well-posedness of the underlying continuous-time fractional system (2.4).

3.1. Existence and uniqueness of the continuous fractional system

Consider the continuous fractional-order system

$$D_t^{\alpha} X(t) = H(X(t)), \qquad X(0) = X_0, \tag{3.1}$$

where

$$X(t) = \begin{bmatrix} L(t) \\ M(t) \\ N(t) \end{bmatrix}, \qquad H(X) = \begin{bmatrix} aL(1-L) - LN + LMN \\ bM(1-M) - MN + LMN \\ \beta LN + qMN - cN^2 \end{bmatrix},$$

with $0 < \alpha \leq 1$ and $X_0 \in \mathbb{R}^3_+$.

Let

$$\Psi = \{(L, M, N) \in \mathbb{R}^3 : \max(|L|, |M|, |N|) \leq \delta\},$$

for some $\delta > 0$. Since the vector field $H(X)$ is continuously differentiable with respect to X on Ψ, it satisfies a local Lipschitz condition on this domain. The fractional system can be written in the equivalent Volterra integral form

$$X(t) = X_0 + \frac{1}{\Gamma(\alpha)} \int_0^t (t - \tau)^{\alpha-1} H(X(\tau))\, d\tau. \tag{3.2}$$

Define the operator

$$Q(X)(t) = X_0 + \frac{1}{\Gamma(\alpha)} \int_0^t (t - \tau)^{\alpha-1} H(X(\tau))\, d\tau.$$

For any $X_1, X_2 \in \Psi$, one obtains the estimate

$$\|Q(X_1) - Q(X_2)\| \leq \frac{T^\alpha}{\Gamma(1 + \alpha)} L_H \|X_1 - X_2\|,$$

where L_H denotes the Lipschitz constant of H on Ψ. Hence, if

$$C = \frac{T^\alpha}{\Gamma(1 + \alpha)} L_H < 1, \tag{3.3}$$

the operator Q is a contraction mapping on Ψ. By Banach's fixed-point theorem, the continuous fractional system admits a unique solution on the interval $(0, T]$. Therefore, the fractional-order ecological model (2.4) is well posed in the sense of existence and uniqueness.

3.2. Well-posedness of the discrete-time fractional map

The discrete-time fractional-order system (2.5) is defined by the recursive mapping

$$(L_{n+1}, M_{n+1}, N_{n+1}) = \mathcal{F}(L_n, M_n, N_n),$$

where $\mathcal{F} : \mathbb{R}^3_+ \to \mathbb{R}^3_+$ is explicitly given by the right-hand side of (2.5). Since $\mathcal{F}$ is continuous and uniquely defined for all $(L_n, M_n, N_n) \in \mathbb{R}^3_+$, it follows that for any initial condition (L_0, M_0, N_0), the sequence $\{(L_n, M_n, N_n)\}_{n\geq 0}$ exists and is unique.

Moreover, for biologically admissible initial values and positive parameters, the mapping $\mathcal{F}$ preserves positivity, that is,

$$L_n > 0, \quad M_n > 0, \quad N_n > 0, \quad \text{for all } n \geq 0,$$

provided that the step size h is sufficiently small. Hence, the discrete fractional predator–prey system (2.5) is well posed as a dynamical system on a positive invariant region.

Consequently, both the continuous fractional prototype and its discrete-time fractional counterpart satisfy standard well-posedness requirements. This guarantees the mathematical consistency and reliability of the subsequent stability, bifurcation, and chaos control analysis [28, 29].

4. Dynamical behavior and stability of the discrete-time fractional predator–prey model

To analyze the local dynamical behavior of system (2.5), the governing equations are linearized in a neighborhood of each equilibrium point. The corresponding Jacobian matrix is then evaluated, and the stability of an equilibrium is determined by examining the moduli of its eigenvalues [30, 31].

Lemma 1. *Let λ_i $(i = 1, 2, 3)$ denote the eigenvalues of the Jacobian matrix of* (2.5) *evaluated at an equilibrium point. Then the equilibrium is classified as follows:*

- *A* sink *if $|\lambda_i| < 1$ for all $i = 1, 2, 3$;*
- *A* source *if $|\lambda_i| > 1$ for all $i = 1, 2, 3$;*
- *A* saddle *if there exists at least one eigenvalue with $|\lambda_i| < 1$ and at least one eigenvalue with $|\lambda_j| > 1$;*
- Non-hyperbolic *if at least one eigenvalue satisfies $|\lambda_i| = 1$.*

The equilibrium points are obtained by imposing the fixed-point conditions $L_{n+1} = L_n$, $M_{n+1} = M_n$, and $N_{n+1} = N_n$ in (2.5). The system admits up to eight biologically meaningful equilibria:

$$E_0 = (0, 0, 0), \quad E_1 = (1, 0, 0), \quad E_2 = (1, 1, 0), \quad E_3 = (0, 1, 0),$$

$$E_4 = (0, cB, qB), \quad E_5 = (cG, 0, \beta G), \quad E_6 = \left(1, 1, \tfrac{\beta+q}{c}\right), \quad E_7 = (L^*, M^*, N^*),$$

where $B = \frac{b}{bc+q}$, $G = \frac{a}{ac+\beta}$, and (L^*, M^*, N^*) denotes the coexistence equilibrium.

I. Trivial and boundary equilibria. The Jacobian matrices at E_0–E_3 are either diagonal or triangular, with eigenvalues depending on a, b, β, and the discretization factor $h^\alpha/\Gamma(1+\alpha)$. In each case, at least one eigenvalue satisfies $|\lambda_i| > 1$, which implies instability. Therefore,

$$E_0, E_1, E_2, E_3 \quad \text{are all unstable (sources or saddles).}$$

II. Semi-interior equilibria. At $E_4 = (0, cB, qB)$ and $E_5 = (cG, 0, \beta G)$, the Jacobian matrices exhibit coupled predator–prey interactions. The characteristic polynomial of each Jacobian contains one decoupled eigenvalue (λ_{41} or λ_{51}) located outside the unit circle, while the remaining two eigenvalues satisfy

$$\lambda^2 - Tr_i\lambda + Det_i = 0, \qquad i = 4, 5,$$

where Tr_i and Det_i denote the trace and determinant of the reduced Jacobian. According to the Schur stability criteria [32],

$$|Det_i| < 1, \qquad 1 \pm Tr_i + Det_i > 0.$$

Violation of any of these inequalities yields either a saddle or a source. Direct substitution confirms that for biologically feasible parameters $(a, b, \beta, q, c > 0)$, the equilibria E_4 and E_5 are generally unstable except for sufficiently small values of h.

III. Interior equilibrium without cooperation. At $E_6 = (1, 1, (\beta + q)/c)$, the Jacobian matrix takes a symmetric form that couples both prey populations. The corresponding eigenvalues are

$$\lambda_{61} = 1 - \tfrac{(\beta+q)h^\alpha}{\Gamma(1+\alpha)}, \qquad \lambda_{62,63} = 1 - \tfrac{h^\alpha}{2\Gamma(1+\alpha)}[a + b \pm \sqrt{\Delta_6}].$$

Hence, E_6 is locally asymptotically stable (a sink) if all eigenvalues satisfy $|\lambda_i| < 1$, that is,

$$0 < h < \min\{h_{61}, h_{62}\}, \qquad h_{6i} = \left(\frac{4\Gamma(1+\alpha)}{a+b\pm\sqrt{\Delta_6}}\right)^{1/\alpha},$$

where

$$\Delta_6 = (a-b)^2 + 4\left(\frac{\beta+q}{c}\right)^2.$$

Increasing the discretization step h causes the eigenvalues to cross the unit circle, leading to oscillatory behavior or bifurcation phenomena [33].

IV. Coexistence equilibrium. The coexistence equilibrium $E_7 = (L^*, M^*, N^*)$ is given by

$$L^* = \frac{bc + q(1-\sqrt{b/a})}{q+\beta\sqrt{b/a}}, \quad M^* = \frac{c\sqrt{ab} - \beta(1-\sqrt{b/a})}{q+\beta\sqrt{b/a}}, \quad N^* = \sqrt{ab},$$

which exists under the feasibility conditions

$$c\sqrt{ab} \le \beta + q, \quad bc + q > q\sqrt{b/a}, \quad ac + \beta > \beta\sqrt{a/b}.$$

Linearization around E_7 yields the cubic characteristic polynomial

$$F(\lambda) = \lambda^3 + k_1\lambda^2 + k_2\lambda + k_3 = 0,$$

where

$$\begin{aligned}
k_1 &= -3 + l_1\frac{h^\alpha}{\Gamma(\alpha+1)},\\
k_2 &= 3 - 2l_1\frac{h^\alpha}{\Gamma(\alpha+1)} + l_2\left(\frac{h^\alpha}{\Gamma(\alpha+1)}\right)^2,\\
k_3 &= -1 + l_1\frac{h^\alpha}{\Gamma(\alpha+1)} - l_2\left(\frac{h^\alpha}{\Gamma(\alpha+1)}\right)^2 + l_3\left(\frac{h^\alpha}{\Gamma(\alpha+1)}\right)^3,
\end{aligned}$$

with

$$\begin{aligned}
l_1 &= aL^* + bM^* + c,\\
l_2 &= \left[\left(ab - (q+\beta)N^* - N^{*2}\right)M^* + ac + \beta N^*\right]L^* + (bc + qN^*)M^*,\\
l_3 &= \Big(\left[(1-L^*)\beta + (1-M^*)q - c\right]N^{*2} + b\beta(1-M^*) + aq(1-L^*)N^* + abc\Big)L^*M^*.
\end{aligned}$$

The Schur–Cohn conditions [34] guarantee that all roots lie inside the unit circle if

$$F(1) > 0, \quad (-1)^3F(-1) > 0, \quad \Delta_2^+ > 0, \quad \Delta_2^- > 0.$$

Although the Schur–Cohn inequalities are expressed in terms of the characteristic polynomial coefficients (k_1, k_2, k_3), these coefficients are explicit functions of the biological parameters (a, b, β, q, c) and the fractional discretization factor $h^\alpha/\Gamma(1+\alpha)$. Therefore, the Schur–Cohn conditions implicitly define admissible regions in the parameter space that guarantee local asymptotic stability of the coexistence equilibrium E_7. In particular, increasing the discretization step h or decreasing the

fractional order α enlarges the effective gain $h^\alpha/\Gamma(1+\alpha)$, which may violate the Schur–Cohn inequalities and induce oscillatory or unstable dynamics. Conversely, smaller values of h and larger values of α favor stability by keeping all characteristic roots inside the unit circle. Hence, the Schur–Cohn conditions translate into biologically meaningful constraints on the sampling scale and memory intensity of the ecosystem.

The coexistence equilibrium E_7 is locally asymptotically stable when these inequalities hold; otherwise, it becomes unstable or undergoes bifurcation as h or α vary [35].

All trivial and boundary equilibria (E_0–E_5) are unstable, whereas the interior equilibria (E_6 and E_7) govern the long-term dynamics. The discrete-time fractional framework reveals that both α and h play critical roles in stability: smaller α or larger h may shift the system from stable coexistence to oscillatory or chaotic behavior. These transitions are further investigated through bifurcation analysis in the next section [36].

5. Bifurcation analysis

In this section, we investigate local bifurcations of the discrete-time fractional-order multi-team predator–prey model (2.5). The interaction coefficient c is selected as the bifurcation parameter, and c_0 denotes a critical value at which the coexistence equilibrium E_7 loses stability through either a flip (period-doubling) or an NS bifurcation. Three bifurcation scenarios are considered: (i) NS bifurcation, (ii) flip bifurcation, and (iii) the codimension-two flip–NS interaction.

5.1. Neimark–Sacker (NS) bifurcation

Let

$$F(\lambda) = \lambda^3 + k_1\lambda^2 + k_2\lambda + k_3$$

be the characteristic polynomial of the Jacobian matrix of (2.5) evaluated at the coexistence equilibrium E_7. The map (2.5) undergoes an NS bifurcation at $c = c_0$ if the following algebraic conditions hold (see, e.g., [37]):

$$\begin{aligned}
&e_1 = \Delta_2^-(c_0) = 0 \iff 1 - k_2 + k_3(k_1 - k_3) = 0,\\
&e_2 = (-1)^3 F_{c_0}(-1) > 0 \iff -k_3 + k_2 - k_1 + 1 > 0,\\
&e_3 = F_{c_0}(1) > 0 \iff k_3 + k_2 + k_1 + 1 > 0,\\
&e_4 = \Delta_2^+(c_0) > 0 \iff 1 + k_2 - k_3(k_1 + k_3) > 0,\\
&e_5 = \frac{d}{dc}\Delta_2^-(c)\Big|_{c=c_0} \neq 0.
\end{aligned} \tag{5.1}$$

Substituting the explicit expressions of k_1, k_2, k_3 obtained in the stability analysis yields the semi-algebraic system

$$\begin{aligned}
e_1 &= -l_3^2\left(\frac{h^\alpha}{\Gamma(\alpha+1)}\right)^6 + 2l_2l_3\left(\frac{h^\alpha}{\Gamma(\alpha+1)}\right)^5 - (l_1l_3 + l_2^2)\left(\frac{h^\alpha}{\Gamma(\alpha+1)}\right)^4 + (l_1l_2 - l_3)\left(\frac{h^\alpha}{\Gamma(\alpha+1)}\right)^3 = 0,\\
e_2 &= -l_3\left(\frac{h^\alpha}{\Gamma(\alpha+1)}\right)^3 + 2l_2\left(\frac{h^\alpha}{\Gamma(\alpha+1)}\right)^2 - 4l_1\frac{h^\alpha}{\Gamma(\alpha+1)} + 8 > 0,
\end{aligned}$$

$$
\begin{aligned}
e_3 &= l_3\left(\frac{h^\alpha}{\Gamma(\alpha+1)}\right)^3 > 0,\\
e_4 &= -l_3^2\left(\frac{h^\alpha}{\Gamma(\alpha+1)}\right)^6 + 2l_2l_3\left(\frac{h^\alpha}{\Gamma(\alpha+1)}\right)^5 - (3l_1l_3 + l_2^2)\left(\frac{h^\alpha}{\Gamma(\alpha+1)}\right)^4 + (3l_1l_2 + 5l_3)\left(\frac{h^\alpha}{\Gamma(\alpha+1)}\right)^3\\
&\quad - 2(l_1^2 + 2l_2)\left(\frac{h^\alpha}{\Gamma(\alpha+1)}\right)^2 + 4l_1\frac{h^\alpha}{\Gamma(\alpha+1)} > 0,\\
e_5 &\neq 0.
\end{aligned} \tag{5.2}
$$

Figure 1 illustrates the NS scenario: the curve $e_1 = 0$ gives the NS threshold in parameter space, while the time series confirms the appearance of quasiperiodic oscillations in the post-bifurcation regime [37].

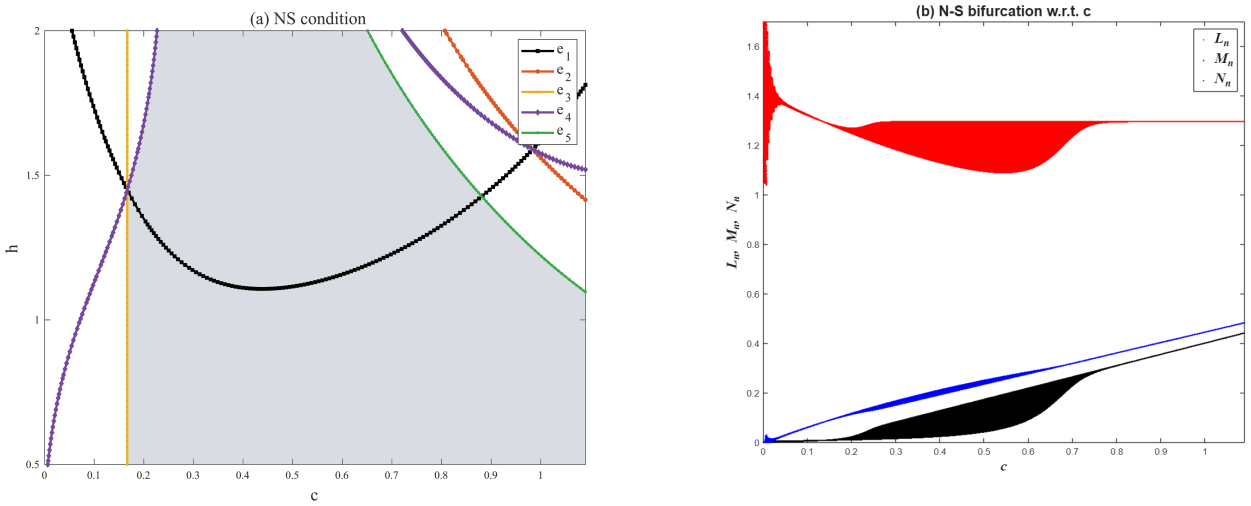

Figure 1. NS bifurcation of the coexistence equilibrium E_7. (a) Parameter region associated with the NS bifurcation conditions in Eq (5.2). The black curve corresponds to $e_1 = 0$ (NS threshold), and the admissible region is determined by inequalities e_2–e_4 together with the transversality condition $e_5 \neq 0$. (b) Representative quasiperiodic oscillations generated after the NS bifurcation of the coexistence equilibrium E_7 (after discarding transients).

5.2. *Flip bifurcation*

A flip (period-doubling) bifurcation occurs when one real multiplier crosses -1. A sufficient algebraic characterization for maps of this type is given in [38]. At $c = c_0$, the flip bifurcation conditions can be written as

$$
\begin{aligned}
b_1 &= F_{c_0}(-1) = 0 \iff k_3 - k_2 + k_1 - 1 = 0,\\
b_2 &= F_{c_0}(1) > 0 \iff k_3 + k_2 + k_1 + 1 > 0,\\
b_3 &= \Delta_2^+(c_0) > 0,\\
b_4 &= \Delta_2^-(c_0) > 0,\\
b_5 &= \frac{d}{dc}(k_1 - k_2 + k_3)\Big|_{c=c_0} \neq 0.
\end{aligned} \tag{5.3}
$$

Substitution yields

$$\begin{aligned} b_1 &= l_3\left(\frac{h^\alpha}{\Gamma(\alpha+1)}\right)^3 - 2l_2\left(\frac{h^\alpha}{\Gamma(\alpha+1)}\right)^2 + 4l_1\frac{h^\alpha}{\Gamma(\alpha+1)} - 8 = 0, \\ b_2 &= l_3\left(\frac{h^\alpha}{\Gamma(\alpha+1)}\right)^3 > 0, \\ b_3 &> 0, \qquad b_4 > 0, \qquad b_5 \neq 0. \end{aligned} \tag{5.4}$$

Figure 2 confirms the flip scenario: the condition $b_1 = 0$ determines the critical threshold, while the numerical results illustrate the emergence of a period-two orbit after the loss of stability [38].

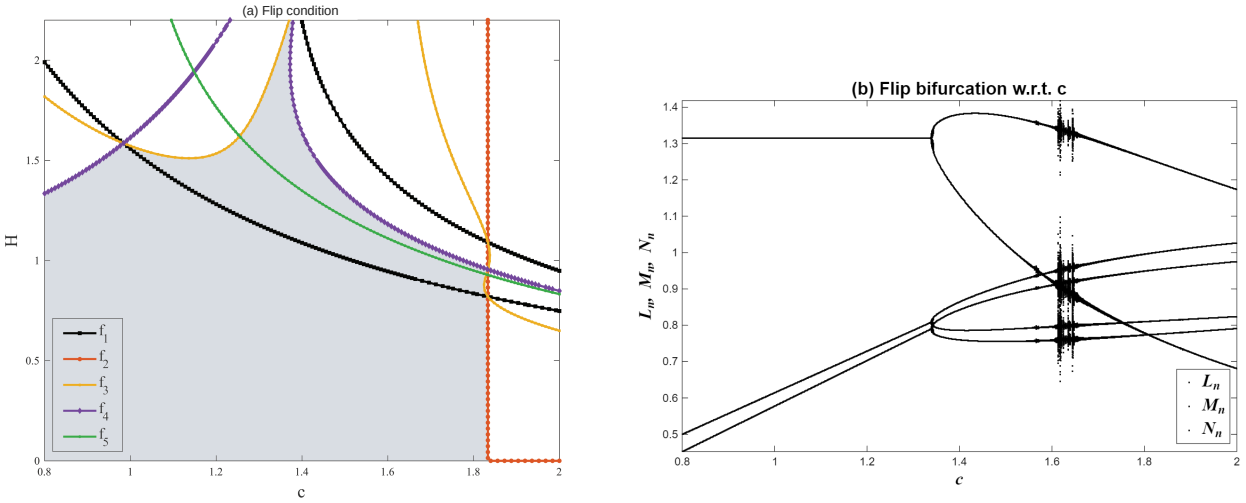

Figure 2. Flip bifurcation of the coexistence equilibrium E_7. (a) Parameter region associated with the flip bifurcation condition. (b) Dynamical behavior of the system after the flip bifurcation, showing the emergence of periodic oscillations.

5.3. *Flip–NS bifurcation and normal form derivation*

A codimension-two flip–NS bifurcation occurs when the Jacobian at E_7 has one real multiplier $\lambda = -1$ and a complex conjugate pair $\lambda_{2,3} = e^{\pm i\theta}$ lying on the unit circle. Following [39], this occurs at $c = c_0$ if

$$\begin{aligned} &p_1 = F_{c_0}(-1) = 0, \quad p_2 = F_{c_0}(1) > 0, \\ &p_3 = 1 - k_3 = 0, \quad p_4 = 1 + k_3 > 0, \quad p_5 = 3 - 2k_1 + k_2 > 0, \\ &p_6 = k_3' \neq 0, \quad p_7 = k_1' - k_2' + k_3' \neq 0, \end{aligned} \tag{5.5}$$

where $(\cdot)'$ denotes differentiation with respect to c.

Expanding these conditions yields

$$\begin{aligned}
&p_1 = l_3\left(\frac{h^\alpha}{\Gamma(\alpha+1)}\right)^3 - 2l_2\left(\frac{h^\alpha}{\Gamma(\alpha+1)}\right)^2 + 4l_1\frac{h^\alpha}{\Gamma(\alpha+1)} - 8 = 0,\\
&p_2 = l_3\left(\frac{h^\alpha}{\Gamma(\alpha+1)}\right)^3 > 0, \quad p_3 = -l_3\left(\frac{h^\alpha}{\Gamma(\alpha+1)}\right)^3 + l_2\left(\frac{h^\alpha}{\Gamma(\alpha+1)}\right)^2 + l_1\frac{h^\alpha}{\Gamma(\alpha+1)} + 2 = 0,\\
&p_4 = l_3\left(\frac{h^\alpha}{\Gamma(\alpha+1)}\right)^3 - l_2\left(\frac{h^\alpha}{\Gamma(\alpha+1)}\right)^2 + l_1\frac{h^\alpha}{\Gamma(\alpha+1)} > 0,\\
&p_5 = l_2\left(\frac{h^\alpha}{\Gamma(\alpha+1)}\right)^2 - 4l_1\frac{h^\alpha}{\Gamma(\alpha+1)} + 12 > 0,\\
&p_{6,7} \neq 0.
\end{aligned} \tag{5.6}$$

Let $X_{n+1} = G(X_n;\mu)$ denote the map induced by (2.5), where $X_n = (L_n, M_n, N_n)^T$ and $\mu = (\mu_1, \mu_2)$ is a two-parameter unfolding with μ_1, μ_2 smooth functions of $(c - c_0)$ and one additional parameter (e.g., h or α). Translate the fixed point to the origin by $Y_n = X_n - E_7$, so that

$$Y_{n+1} = AY_n + F(Y_n;\mu), \qquad A = DG(E_7;\mu)\big|_{\mu=0},$$

where A has eigenvalues -1 and $e^{\pm i\theta}$. Let E^c denote the three-dimensional center subspace spanned by the corresponding eigenvectors. By the center manifold theorem, there exists a locally invariant center manifold $\mathcal{W}^c$ tangent to E^c at the origin, and the local dynamics are governed by the restriction of the map to $\mathcal{W}^c$.

Choose real/complex coordinates $(u, z) \in \mathbb{R} \times \mathbb{C}$ on E^c such that u corresponds to the flip direction and z corresponds to the NS pair. After solving the center manifold invariance equation up to third order and performing standard near-identity transformations [34], the reduced map can be written in the qualitative flip–NS normal form

$$\begin{aligned}
u_{n+1} &= -u_n + \mu_1 + a_{20}u_n^2 + a_{02}|z_n|^2 + O(\|(u_n, z_n)\|^3),\\
z_{n+1} &= e^{i\theta}z_n\Big(1 + \mu_2 + b_{11}u_n + b_{21}u_n^2 + b_{03}|z_n|^2\Big) + O(\|(u_n, z_n)\|^3).
\end{aligned} \tag{5.7}$$

Here $\theta \in (0, \pi)$ is determined by the critical pair $e^{\pm i\theta}$, and the coefficients $a_{20}, a_{02}, b_{11}, b_{21}, b_{03}$ are computable functions of the second and third derivatives of G at E_7 (multilinear forms on eigenvectors), as is standard in codimension-two bifurcation theory [34, 39]. The nondegeneracy and transversality assumptions required for the validity of the unfolding are ensured in our case by the conditions $p_6 \neq 0$ and $p_7 \neq 0$, which prevent tangential crossing and guarantee that the critical multipliers cross the unit circle with nonzero speed. The normal form (5.7) explains the local coexistence and interaction of period-doubling (u-direction) and quasiperiodic (z-direction) dynamics near the codimension-two point.

Figure 3 shows the parameter sets where the algebraic flip–NS conditions hold: the curves $p_1 = 0$ (flip boundary) and $p_3 = 0$ (NS boundary) intersect within the admissible region defined by p_2, p_4, and p_5. This intersection defines the codimension-two point where flip and NS bifurcations coincide, confirming the flip–NS bifurcation [39].

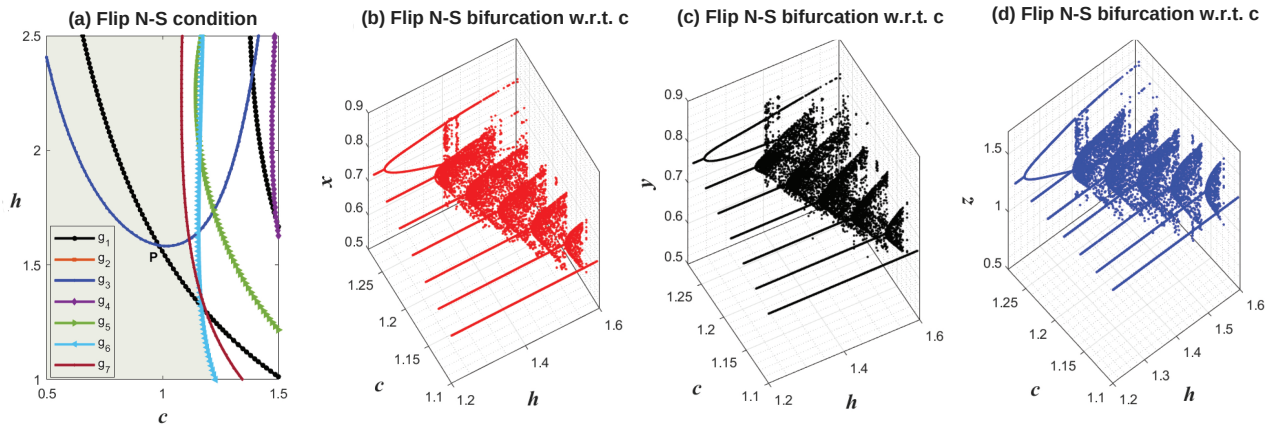

Figure 3. Codimension-two flip–NS bifurcation in Model (2.5). (a) The curves $p_1 = 0$ and $p_3 = 0$ (Eq (5.6)) intersect inside the admissible region defined by inequalities p_2, p_4, and p_5, confirming the flip–NS interaction point. (b)–(d) Flip–NS bifurcation behavior with respect to the parameter c, illustrating the emergence of complex dynamics in the state variables and confirming the coexistence of flip and NS bifurcations.

6. Numerical simulation

In this section, the dynamical behavior of Model (2.5) is investigated numerically to illustrate the analytical findings obtained in the preceding sections. Since closed-form solutions of fractional-order discrete systems are generally unavailable, numerical iteration is used to explore bifurcation structure and chaotic dynamics. Unless stated otherwise, the fixed parameters are $a = q = 1.2$, $\beta = 1$, and the initial condition is $(L_0, M_0, N_0) = (0.2, 0.4, 0.6)$. The fractional order and step size are taken as $\alpha = 0.85$ and $h = 1.04$ throughout this section.

6.1. Numerical bifurcation behavior

In the first numerical experiment, parameters are chosen so that the semi-algebraic conditions in (5.2) are satisfied for $c \in (0, 1.5)$. By substituting the prescribed parameters into the NS threshold equation $e_1 = 0$ in (5.2), the critical value associated with the onset of an NS bifurcation is obtained as

$$c_* = 0.273, \qquad E_7 = (0.0638,\ 0.22,\ 1.2).$$

As depicted in Figure 1, the equilibrium E_7 is stable for $c > c_*$, while a loss of stability occurs through an NS bifurcation when $c < c_*$, giving rise to quasiperiodic oscillations.

Similarly, when the parameters satisfy the flip-bifurcation conditions in (5.4) for $c \in (1.2, 1.4)$, substitution into the flip threshold equation $b_1 = 0$ yields the critical value

$$c_{**} = 1.339.$$

As shown in Figure 2, the equilibrium E_7 remains stable for $c < c_{**}$ but undergoes a flip (period-doubling) bifurcation when $c > c_{**}$. A representative phase portrait at $c = 1.8$ is displayed in Figure 4, illustrating the transition to a complex oscillatory regime.

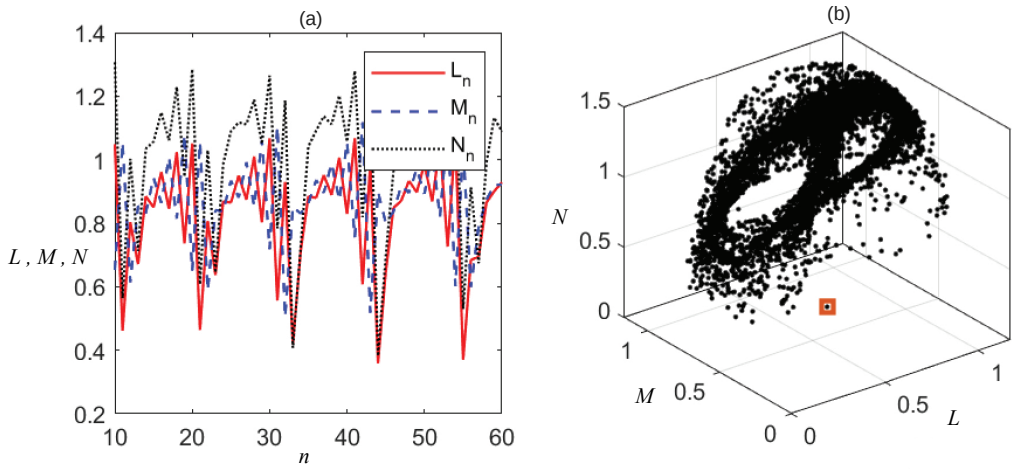

Figure 4. Phase portrait of Model (2.5) at $c = 1.8$, with $\alpha = 0.85$, $h = 1.04$, $a = q = 1.2$, and $\beta = 1$. The red circle marks the initial condition. (a) Time series of the variables L_n, M_n, and N_n. (b) Corresponding phase portrait in the three-dimensional state space.

6.2. Chaos detection via the 0–1 test

To detect the emergence of chaotic behavior, the 0–1 test for chaos is employed as a diagnostic tool to distinguish regular and irregular motions. The test is based on the asymptotic growth of the translational variables $(P_{c^*}(n), Q_{c^*}(n))$ constructed from the observable sequence N_n. The numerical outcomes for two representative parameter values are shown in Figures 5 and 6.

For $c = 1$, the test yields an asymptotic growth rate $K = 0.1414 \approx 0$, indicating regular behavior. The trajectories in the $(P_{c^*}(n), Q_{c^*}(n))$ plane remain bounded (see Figure 5), confirming a non-chaotic regime.

In contrast, for $c = 1.625$, the test gives $K = 0.655 \approx 1$, revealing chaotic dynamics. The corresponding trajectories (see Figure 6) display Brownian-like diffusion, which is characteristic of chaos. The dependence of K and the mean-square displacement $M_{c^*}(n)$ further supports that values $K \approx 0$ correspond to regular motion, whereas values close to unity indicate chaotic motion.

The numerical simulations support the theoretical bifurcation analysis. The system exhibits an NS bifurcation at $c_* = 0.273$, followed by a flip bifurcation at $c_{**} = 1.339$, leading to quasiperiodic and chaotic oscillations, respectively. The 0–1 test and phase-space trajectories validate the coexistence of regular and chaotic regimes depending on the bifurcation parameter c, and confirm that the fractional-order setting enriches the nonlinear dynamics and enlarges the parameter ranges supporting complex oscillations.

The evolution of the system dynamics beyond the flip bifurcation is further illustrated in Figure 7. As the parameter c increases, the system transitions from a stable equilibrium to periodic oscillations and eventually to chaotic behavior, as shown in the corresponding phase portraits.

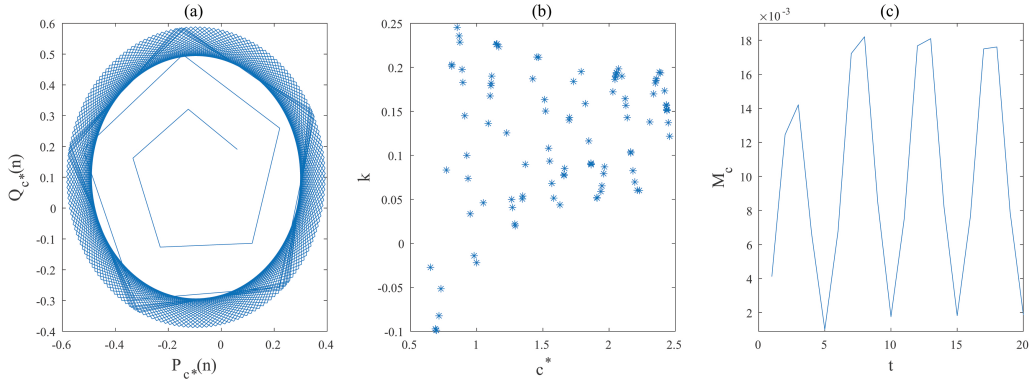

Figure 5. 0–1 test for chaos for the observable N_n at $c = 1$ (regular regime). The trajectory in the $(P_c^*(n), Q_c^*(n))$ plane remains bounded and the corresponding growth rate satisfies $K \approx 0$. (a) Trajectory of $(P_c^*(n), Q_c^*(n))$. (b) Evolution of the growth rate K. (c) Mean-square displacement $M_c^*(n)$ confirming regular (non-chaotic) dynamics.

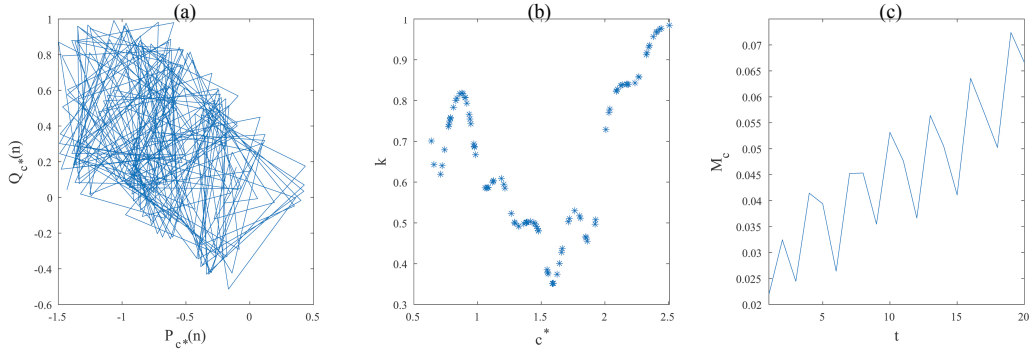

Figure 6. 0–1 test for chaos for the observable N_n at $c = 1.625$ (chaotic regime). The $(P_c^*(n), Q_c^*(n))$ trajectory exhibits Brownian-like diffusion and the corresponding growth rate indicates $K \approx 1$. (a) Trajectory of $(P_c^*(n), Q_c^*(n))$. (b) Evolution of the growth rate K. (c) Mean-square displacement $M_c^*(n)$ confirming chaotic dynamics.

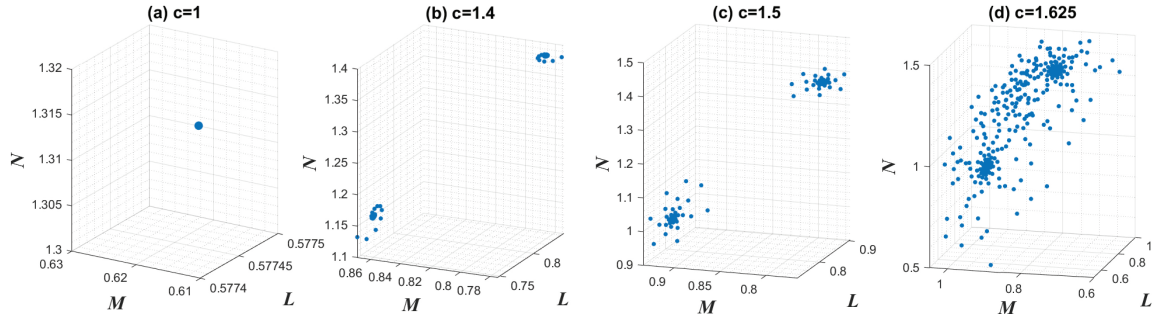

Figure 7. Phase portraits of Model (2.5) illustrating the post-flip bifurcation dynamics as the bifurcation parameter c increases. (a) Stable equilibrium at $c = 1$. (b) Periodic oscillations at $c = 1.4$ after the onset of bifurcation. (c) More pronounced oscillatory behavior at $c = 1.5$, indicating further development of the post-bifurcation dynamics. (d) Chaotic attractor at $c = 1.625$. These phase portraits show the transition from a stable fixed point to periodic motion and finally to chaos as c increases.

7. Chaos control

The control of chaotic oscillations and bifurcations in discrete-time biological systems is a critical issue in population management and stability analysis. Even small parameter perturbations may drive the system into unpredictable or biologically undesirable regimes. Therefore, suitable control mechanisms are required to stabilize unstable periodic orbits and restore biologically meaningful equilibria [40]. In this section, three control strategies are applied to Model (2.5): (i) the OGY feedback control method, (ii) a hybrid control technique based on a convex combination scheme, and (iii) a state feedback control scheme for robust stabilization.

7.1. The Ott–Grebogi–Yorke (OGY) control method

We first apply the classical OGY control approach proposed by Ott et al. [41], which stabilizes chaotic trajectories by introducing small perturbations to a chosen system parameter. Let c be the controlled parameter in Model (2.5). The map can be written componentwise as

$$\begin{aligned} L_{n+1} &= L_n + \tfrac{h^\alpha}{\Gamma(\alpha+1)}\,[aL_n(1-L_n) - L_nN_n + L_nM_nN_n] = f(L_n, M_n, N_n),\\ M_{n+1} &= M_n + \tfrac{h^\alpha}{\Gamma(\alpha+1)}\,[bM_n(1-M_n) - M_nN_n + L_nM_nN_n] = g(L_n, M_n, N_n),\\ N_{n+1} &= N_n + \tfrac{h^\alpha}{\Gamma(\alpha+1)}\left[\beta L_nN_n + qM_nN_n - cN_n^2\right] = s(L_n, M_n, N_n, c), \end{aligned} \tag{7.1}$$

where $c \in (c_0 - \delta, c_0 + \delta)$, c_0 denotes the nominal chaotic value of the parameter, and $\delta > 0$ is a prescribed perturbation bound.

The coexistence equilibrium is $E_7 = (L^*, M^*, N^*)$. Linearizing (7.1) around E_7 yields

$$\begin{bmatrix} L_{n+1} - L^* \\ M_{n+1} - M^* \\ N_{n+1} - N^* \end{bmatrix} \simeq J(L^*, M^*, N^*, c_0) \begin{bmatrix} L_n - L^* \\ M_n - M^* \\ N_n - N^* \end{bmatrix} + K(c - c_0), \tag{7.2}$$

where J is the Jacobian matrix at E_7 evaluated at $c = c_0$ and K is the corresponding control vector.

Let

$$c - c_0 = -R \begin{bmatrix} L_n - L^* \\ M_n - M^* \\ N_n - N^* \end{bmatrix}, \qquad R = [\rho_1, \rho_2, \rho_3],$$

where $\rho_1, \rho_2, \rho_3 \in \mathbb{R}$ are the OGY feedback gains. Then the controlled linearized system becomes

$$\begin{bmatrix} L_{n+1} - L^* \\ M_{n+1} - M^* \\ N_{n+1} - N^* \end{bmatrix} \simeq (J - KR) \begin{bmatrix} L_n - L^* \\ M_n - M^* \\ N_n - N^* \end{bmatrix}. \tag{7.3}$$

The equilibrium E_7 is locally asymptotically stable if all eigenvalues of the matrix $J - KR$ lie strictly inside the open unit disk. The Jury stability criterion provides the corresponding set of algebraic inequalities defining an admissible domain for the feedback gains (ρ_1, ρ_2, ρ_3). Numerical iteration confirms that suitable choices of ρ_i suppress chaotic oscillations (see Figures 8 and 9).

The gains (ρ_1, ρ_2, ρ_3) are chosen so that the Jury inequalities for the controlled Jacobian matrix $J - KR$ are satisfied, ensuring that all eigenvalues lie within the unit circle. No optimization procedure

is used; the aim is feasibility of local asymptotic stabilization under small admissible parameter perturbations.

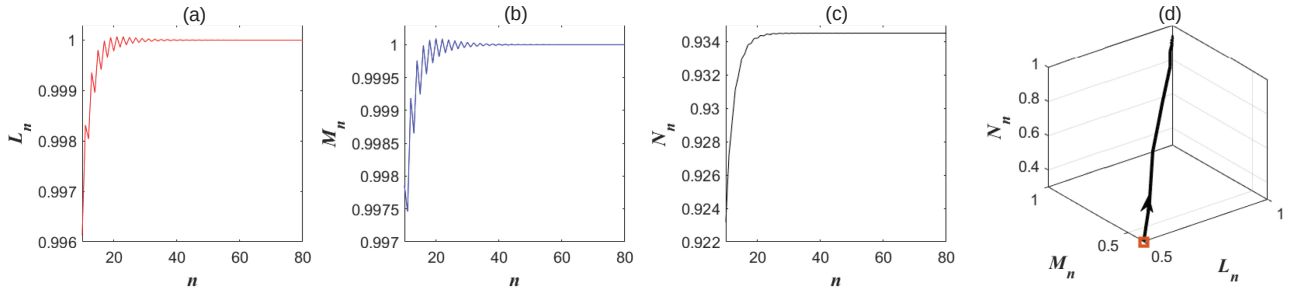

Figure 8. OGY-controlled dynamics of Model (2.5) inside the admissible stability region for $(\alpha, h, c_0, \rho_1, \rho_2, \rho_3) = (0.95, 0.8, 1.2, 0, 1.5, 0.5)$. (a) Time evolution of L_n showing convergence to its equilibrium value. (b) Time evolution of M_n showing convergence to its equilibrium value. (c) Time evolution of N_n showing convergence to its equilibrium value. (d) Three-dimensional phase portrait confirming that the controlled trajectory converges to the coexistence equilibrium under OGY control.

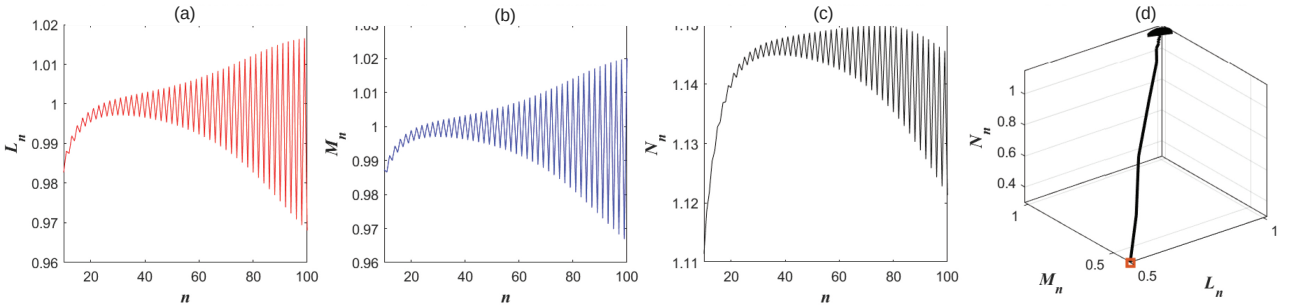

Figure 9. Unstable configuration of the controlled system outside the admissible stability region at $(\alpha, h, c_0, \rho_1, \rho_2, \rho_3) = (0.95, 0.8, 1.2, 0, 0.8, 1.2)$. (a) Time evolution of L_n showing divergence from the equilibrium state. (b) Time evolution of M_n exhibiting unstable oscillatory behavior. (c) Time evolution of N_n indicating loss of stabilization. (d) Three-dimensional phase portrait in the (L, M, N) space illustrating the unstable trajectory and failure of control.

7.2. Hybrid control method

The hybrid control scheme combines the original map and the identity map through a convex combination, thereby reducing the effective nonlinear gain and suppressing chaos generated near flip or NS bifurcation thresholds [42, 43]. The controlled system is defined by

$$\begin{aligned} L_{n+1} &= \rho\Big(L_n + \tfrac{h^\alpha}{\Gamma(\alpha+1)}[aL_n(1-L_n) - L_nN_n + L_nM_nN_n]\Big) + (1-\rho)L_n, \\ M_{n+1} &= \rho\Big(M_n + \tfrac{h^\alpha}{\Gamma(\alpha+1)}[bM_n(1-M_n) - M_nN_n + L_nM_nN_n]\Big) + (1-\rho)M_n, \\ N_{n+1} &= \rho\Big(N_n + \tfrac{h^\alpha}{\Gamma(\alpha+1)}[\beta L_nN_n + qM_nN_n - cN_n^2]\Big) + (1-\rho)N_n, \end{aligned} \tag{7.4}$$

where $0 < \rho < 1$ represents the hybrid control intensity.

By varying ρ, the bifurcation onset can be delayed or eliminated. The admissible range of ρ can be characterized via the Jury stability test applied to the controlled Jacobian matrix.

The parameter ρ acts as a convex combination factor between the original system dynamics and the stabilizing identity map. Its feasible range is determined through Jury stability conditions rather than through performance optimization.

The effectiveness of the hybrid control strategy in suppressing chaotic oscillations and stabilizing the system dynamics is illustrated in Figure 10. It is evident that the controlled trajectories converge toward the coexistence equilibrium, confirming the efficiency of the hybrid control approach.

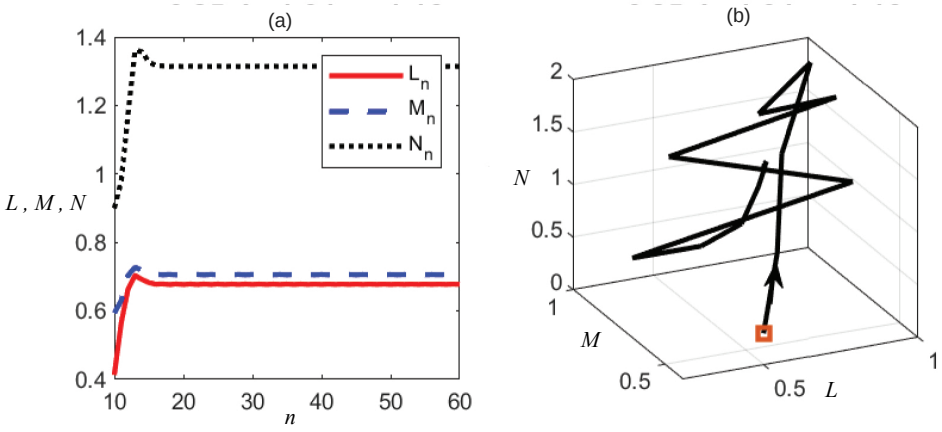

Figure 10. Phase portrait of Model (2.5) under hybrid control with $\alpha = 0.85$ and $h = 1.04$, illustrating the suppression of irregular oscillations and the emergence of stabilized behavior. (a) Time evolution of the controlled system variables showing convergence toward the coexistence equilibrium. (b) Phase portrait in the (L, M, N) space demonstrating stabilization of trajectories under hybrid control.

7.3. State feedback control

Finally, a state feedback control strategy [44] is implemented using gains j_1, j_2, j_3. The controlled system takes the form

$$\begin{aligned} L_{n+1} &= L_n + \tfrac{h^\alpha}{\Gamma(\alpha+1)}[aL_n(1-L_n) - L_nN_n + L_nM_nN_n] - j_1(L_n - L^*), \\ M_{n+1} &= M_n + \tfrac{h^\alpha}{\Gamma(\alpha+1)}[bM_n(1-M_n) - M_nN_n + L_nM_nN_n] - j_2(M_n - M^*), \\ N_{n+1} &= N_n + \tfrac{h^\alpha}{\Gamma(\alpha+1)}[\beta L_nN_n + qM_nN_n - cN_n^2] - j_3(N_n - N^*), \end{aligned} \tag{7.5}$$

where the gains are selected such that all eigenvalues of the controlled Jacobian matrix lie inside the unit disk according to the Jury conditions. This guarantees asymptotic stabilization of the coexistence equilibrium E_7 and suppression of irregular oscillations.

The gains (j_1, j_2, j_3) are determined from stability feasibility requirements imposed by the Jury criterion and are not obtained through an optimization procedure.

Similarly, the performance of the state feedback control strategy is demonstrated in Figure 11, where the system trajectories converge toward the coexistence equilibrium after control is applied.

This confirms the capability of state feedback control to effectively stabilize the system and eliminate irregular oscillations.

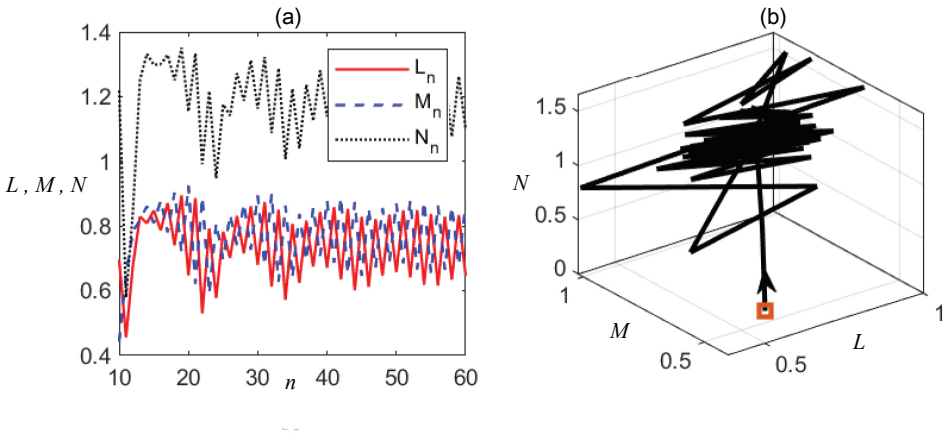

Figure 11. Dynamics of Model (2.5) under state feedback control at $c = 1.4$. The red circle denotes the initial condition, and the trajectory converges toward the coexistence equilibrium after control is applied. (a) Time evolution of the state variables illustrating convergence to equilibrium. (b) Phase portrait in the (L, M, N) space demonstrating stabilization of the controlled trajectory.

To provide a comparative evaluation of the proposed chaos control methods, we summarize their qualitative performance in terms of convergence speed, control effort, and robustness in Table 1. The convergence speed refers to the number of iterations required for trajectories to approach the coexistence equilibrium, the control effort reflects the magnitude of parameter or state perturbations applied, and robustness indicates the sensitivity of each method to parameter variations.

Table 1. Qualitative comparison of chaos control strategies.

Control method	Convergence speed	Control effort	Robustness
OGY feedback control	Moderate	Low	Moderate
Hybrid control	Fast	Moderate	High
State feedback control	Fast	High	High

The results indicate that the OGY method achieves stabilization using minimal parameter perturbations, but typically requires more iterations to converge. The hybrid control scheme exhibits faster convergence and improved robustness near bifurcation thresholds. The state feedback control strategy provides strong stabilization capability, but at the cost of higher control effort due to direct state regulation. These findings suggest a trade-off between convergence speed, robustness, and control intensity when selecting an appropriate chaos control mechanism for discrete fractional ecological systems.

8. Discussion and conclusions

The comparative results indicate that the OGY method achieves stabilization through small admissible parameter perturbations, the hybrid control scheme provides robust chaos suppression in the vicinity of bifurcation thresholds, and the state feedback strategy guarantees local asymptotic stabilization of chaotic dynamics via suitable gain selection. Together, these control approaches form an effective and flexible framework for suppressing chaos and restoring regular behavior in discrete-time fractional biological systems, in agreement with the theoretical stability and bifurcation analysis.

This study presented and analyzed a discrete-time multi-team predator–prey model incorporating fractional-order memory with constant system parameters. The existence of biologically admissible equilibrium states and their local stability characteristics were rigorously examined. Precise analytical criteria for the emergence of NS, flip, and codimension-two flip–NS bifurcations around the coexistence equilibrium E_7 were established. The proposed model is capable of generating a rich spectrum of nonlinear dynamical responses, including periodic cycles, quasiperiodic motion, and chaotic attractors. The validity of the theoretical analysis was supported by the 0–1 chaos test and numerical simulations, which clearly demonstrated transitions between regular and chaotic dynamics.

From a biological perspective, the fractional-order parameter α provides an effective mathematical representation of long-term ecological memory arising from repeated predator–prey interactions, adaptive behavioral responses, and cumulative environmental effects. In particular, smaller values of α correspond to stronger memory effects, meaning that current population growth depends more heavily on past states, while $\alpha \to 1$ recovers the classical memory-free discrete model. Numerical simulations indicate that variations in α modify stability thresholds and bifurcation boundaries, thereby reshaping the parameter regions associated with stable coexistence, oscillations, and chaos. Ecologically, this implies that memory mechanisms can act as stabilizing or destabilizing factors depending on their intensity, directly affecting predictability, resilience, and long-term persistence of interacting species. The bifurcation scenarios identified in this study therefore show that fractional memory is not merely a mathematical generalization, but a biologically meaningful control parameter governing the qualitative organization of ecosystem dynamics.

Compared with classical integer-order discrete predator–prey systems, fractional-order models incorporate nonlocal memory effects and thus provide a richer and more realistic description of population interactions. Although parameter estimation and biological interpretation may become more demanding, the fractional framework can capture complex temporal patterns such as alternating regular–chaotic transitions, persistent oscillations, and long-term dynamical correlations that are often observed in real ecological systems.

It is emphasized that the chaos control strategies investigated in this work were intended to demonstrate stabilization feasibility rather than optimal performance. Future research will focus on energy-efficient and robustness-oriented control designs based on optimal control theory, linear matrix inequalities, and data-driven system identification techniques.

In conclusion, the proposed fractional discrete predator–prey model demonstrates that the fractional order plays a decisive role in shaping the system's dynamical evolution. By appropriately tuning the memory parameter, the onset of chaos can be delayed or suppressed and unstable population oscillations can be stabilized. These results contribute to the theoretical understanding of nonlinear ecological dynamics and provide a quantitative foundation for developing practical strategies aimed at

enhancing ecosystem stability and resilience.

Author contributions

Conceptualization: Ibrahim M. E. Abdelsatar, Mahmoud A. M. Abdelaziz, A. A. Al Qarni; Methodology: Ibrahim M. E. Abdelsatar, Mahmoud A. M. Abdelaziz, Elhadi E. Elamir, A. A. Al Qarni; Formal analysis: Ibrahim M. E. Abdelsatar, Mahmoud A. M. Abdelaziz; Software: Mahmoud A. M. Abdelaziz, Ibrahim M. E. Abdelsatar; Writing – original draft: Mahmoud A. M. Abdelaziz, A. A. Al Qarni, Ibrahim M. E. Abdelsatar, Elhadi E. Elamir; Writing – review and editing: Mahmoud A. M. Abdelaziz, Ibrahim M. E. Abdelsatar, Elhadi E. Elamir, A. A. Elsadany, Manal Alqhtani, Montaser O. S. Hilal; Investigation: A. A. Elsadany; Project administration: Mahmoud A. M. Abdelaziz, Elhadi E. Elamir. All authors have read and approved the final version of the manuscript for publication.

Use of Generative-AI tools declaration

The authors acknowledge the use of generative artificial intelligence (AI) tools for the purpose of linguistic refinement, including grammar correction and enhancement of clarity. These tools were not used in the generation of scientific ideas, mathematical modeling, data analysis, or interpretation of results. All intellectual and scientific contributions presented in this manuscript are exclusively those of the authors.

Acknowledgments

The authors are thankful to the Deanship of Graduate Studies and Scientific Research at Najran University for funding this work under the Consortium Funding Program grant code (NU/CPL/SERC/14/4273-1).

Conflict of interest

The authors declare that they have no competing interests.

References

1. A. Suryanto, I. Darti, E. Cahyono, Bifurcation analysis and chaos control of a discrete–time fractional-order predator–prey model with Holling type II functional response and harvesting, *Chaos Theory Appl.*, **7** (2025), 87–98. https://doi.org/10.51537/chaos.1581247
2. S. H. Strogatz, *Nonlinear dynamics and chaos*, With Applications to Physics, Biology, Chemistry, and Engineering, 2 Eds., Westview Press, 2015. https://doi.org/10.1201/9780429492563
3. L. J. Ontañón-García, J. G. Barajas-Ramírez, E. Campos-Cantón, D. A. Magallón-García, C. A. Guerra-García, J. R. Cuesta-García, et al., Algorithm for generating bifurcation diagrams using Poincaré intersection plane, *Mathematics,* **13** (2025), 1818. https://doi.org/10.3390/math13111818

4. M. C. Köhnke, I. Siekmann, H. Malchow, Taxis-driven pattern formation in a predator-prey model with group defense, *Ecol. Complex.*, **43** (2020), 100848. https://doi.org/10.1016/j.ecocom.2020.100848
5. Y. Du, B. Niu, J. Wei, A predator–prey model with cooperative hunting in the predator and group defense in the prey, *Discrete Contin. Dyn. Syst. Ser. B*, **27** (2022), 5845–5881. https://doi.org/10.3934/dcdsb.2021298
6. Y. Enatsu, J. Roy, M. Banerjee, Hunting cooperation in a prey–predator model with maturation delay, *J. Biol. Dyn.*, **18** (2024), 2332279. https://doi.org/10.1080/17513758.2024.2332279
7. E. A. McGehee, N. Schutt, D. A. Vasquez, E. Peacock-Lopez, Bifurcations, and temporal and spatial patterns of a modified Lotka–Volterra model, *Int. J. Bifurcation Chaos*, **18** (2008), 2223–2248. https://doi.org/10.1142/S0218127408021671
8. M. F. Elettreby, Two-prey one-predator model, *Chaos Soliton. Fract.*, **39** (2009), 2018–2027. https://doi.org/10.1016/j.chaos.2007.06.058
9. M. A. M. Abdelaziz, A. I. Ismail, F. A. Abdullah, M. H. Mohd, Discrete-time fractional order SIR epidemic model with saturated treatment function, *Int. J. Nonlinear Sci. Numer. Simul.*, **21** (2020), 397–424. https://doi.org/10.1515/ijnsns-2019-0068
10. J. Roy, S. Dey, B. W. Kooi, M. Banerjee, Prey group defense and hunting cooperation among generalist-predators induce complex dynamics: a mathematical study, *J. Math. Biol.*, **89** (2024), 22. https://doi.org/10.1007/s00285-024-02121-9
11. H. Chen, M. Liu, X. Xu, Dynamics of a prey–predator model with group defense for prey, cooperative hunting for predator, and Lévy jump, *Axioms*, **12** (2023), 878. https://doi.org/10.3390/axioms12090878
12. S. Patnaik, J. P. Hollkamp, F. Semperlotti, Applications of variable-order fractional operators: a review, *Proc. R. Soc. A*, **476** (2020), 20190498. https://doi.org/10.1098/rspa.2019.0498
13. Q. Din, Stability, bifurcation analysis and chaos control for a predator–prey system, *J. Vib. Control*, **25** (2019), 612–626. https://doi.org/10.1177/1077546318790871
14. A. Deshpande, V. Daftardar-Gejji, Chaos in discrete fractional difference equations, *Pramana – J. Phys.*, **87** (2025), 49. https://doi.org/10.1007/s12043-016-1231-9
15. J. Tenreiro Machado, V. Kiryakova, F. Mainardi, Recent history of fractional calculus, *Commun. Nonlinear Sci. Numer. Simul.*, **16** (2011), 1140–1153. https://doi.org/10.1016/j.cnsns.2010.05.027
16. C. Li, F. Zeng, *Numerical methods for fractional calculus*, 1 Ed., Chapman and Hall/CRC, 2015. https://doi.org/10.1201/b18503
17. K. Diethelm, *The analysis of fractional differential equations*, An Application-Oriented Exposition Using Differential Operators of Caputo Type, Vol. 200, Springer Berlin, 2010. https://doi.org/10.1007/978-3-642-14574-2
18. M. Singh, M. P. Singh, M. Tamsir, M. Asif, Analysis of fractional-order nonlinear dynamical systems by using different techniques, *Int. J. Appl. Comput. Math.*, **11** (2025), 47. https://doi.org/10.1007/s40819-025-01865-2
19. L. Li, J. G. Liu, A generalized definition of Caputo derivatives and its application to fractional ODEs, *SIAM J. Math. Anal.*, **50** (2018), 2867–2900. https://doi.org/10.1137/17M1160318

20. E. Rahmi, N. Anggriani, H. S. Panigoro, O. J. Peter, A fractional-order approach to predator–prey interactions: Modeling fear and disease dynamics with memory effects, *PLoS One*, **21** (2026), e0339351. https://doi.org/10.1371/journal.pone.0339351

21. C. Ionescu, A. Lopes, D. Copot, J. A. T. Machado, J. H. T. Bates, The role of fractional calculus in modeling biological phenomena: a review, *Commun. Nonlinear Sci. Numer. Simul.*, **51** (2017), 141–159. https://doi.org/10.1016/j.cnsns.2017.04.001

22. R. Hilfer, *Applications of fractional calculus in physics*, World Scientific, 2000. https://doi.org/10.1142/3779

23. M. Rayungsari, A. Suryanto, W. M. Kusumawinahyu, I. Darti, Dynamics analysis of a predator–prey fractional-order model incorporating predator cannibalism and refuge, *Front. Appl. Math. Stat.*, **9** (2023), 1122330. https://doi.org/10.3389/fams.2023.1122330

24. M. Caputo, Linear models of dissipation whose Q is almost frequency independent–II, *Geophys. J. Int.*, **13** (1967), 529–539. https://doi.org/10.1111/j.1365-246X.1967.tb02303.x

25. M. A. Abdelaziz, A. I. Ismail, F. A. Abdullah, M. H. Mohd, Bifurcations and chaos in a discrete SI epidemic model with fractional order, *Adv. Differ. Equ.*, **2018** (2018), 44. https://doi.org/10.1186/s13662-018-1481-6

26. S. Salahshour, T. Allahviranloo, S. Abbasbandy, D. Baleanu, Existence and uniqueness results for fractional differential equations with uncertainty, *Adv. Differ. Equ.*, **2012** (2012), 112. https://doi.org/10.1186/1687-1847-2012-112

27. Y. Kao, C. Wang, H. Xia, Y. Cao, *Analysis and control for fractional-order systems*, Singapore: Springer, 2024. https://doi.org/10.1007/978-981-99-6054-5

28. I. Alraddadi, R. Perumal, R. Ahmed, J. Khan, Y. Lee, Stability and bifurcation analysis of a fractional-order prey–predator model with ratio-dependent functional response, *AIMS Math.*, **11** (2026), 1412–1448. https://doi.org/10.3934/math.2026060

29. A. A. Elsadany, Y. Sabbar, W. Adel, A. El-Mesady, Dynamics of a novel discrete fractional model for maize streak epidemics with linear control, *Int. J. Dyn. Control*, **13** (2025), 5. https://doi.org/10.1007/s40435-024-01509-1

30. S. Elaydi, *An introduction to difference equations*, 3 Eds., New York: Springer, 2005. https://doi.org/10.1007/0-387-27602-5

31. S. Wiggins, *Introduction to applied nonlinear dynamical systems and chaos*, Vol. 2, New York: Springer, 2003. https://doi.org/10.1007/b97481

32. L. E. Garza, N. Martínez, G. Romero, New stability criteria for discrete linear systems based on orthogonal polynomials, *Mathematics*, **8** (2020), 1322. https://doi.org/10.3390/math8081322

33. Q. Din, A. A. Elsadany, H. Khalil, Neimark–Sacker bifurcation and chaos control in a fractional-order plant–herbivore model, *Discrete Dyn. Nat. Soc.*, **2017** (2017), 6312964. https://doi.org/10.1155/2017/6312964

34. H. Kielhöfer, *Bifurcation theory*, Springer, New York, 2012. https://doi.org/10.1007/978-1-4614-0502-3

35. S. F. Aldosary, R. Ahmed, Stability and bifurcation analysis of a discrete Leslie predator-prey system via piecewise constant argument method, *AIMS Math.*, **9** (2024), 4684–4706. https://doi.org/10.3934/math.2024226

36. A. Al Khabyah, R. Ahmed, M. S. Akram, S. Akhtar, Stability, bifurcation, and chaos control in a discrete predator-prey model with strong Allee effect, *AIMS Math.*, **8** (2023), 8060–8081. https://doi.org/10.3934/math.2023408

37. S. Shoyimardonov, Neimark-Sacker bifurcation and stability analysis in a discrete phytoplankton-zooplankton system with Holling type II functional response, *J. Appl. Anal. Comput.*, **13** (2023), 2048–2064. https://doi.org/10.11948/20220345

38. B. Xie, Z. Zhang, N. Zhang, Dynamic analysis of a fractional-order three-dimensional predator–prey system with competitive and fear effects, *Nonlinear Dyn.*, **113** (2025), 26949–26979. https://doi.org/10.1007/s11071-025-11499-0

39. M. A. M. Abdelaziz, A. I. Ismail, F. A. Abdullah, M. H. Mohd, Codimension one and two bifurcations of a discrete–time fractional-order SEIR measles epidemic model with constant vaccination, *Chaos Soliton. Fract.*, **140** (2020), 110104. https://doi.org/10.1016/j.chaos.2020.110104

40. R. Saadeh, A. Abbes, A. Al-Husban, A. Ouannas, G. Grassi, The fractional discrete predator–prey model: chaos, control and synchronization, *Fractal Fract.,* **7** (2023), 120. https://doi.org/10.3390/fractalfract7020120

41. E. Ott, C. Grebogi, J. A. Yorke, Controlling chaos, *Phys. Rev. Lett.*, **64** (1990), 1196–1199. https://doi.org/10.1103/PhysRevLett.64.1196

42. X. S. Luo, G. Chen, B. H. Wang, J. Q. Fang, Hybrid control of period-doubling bifurcation and chaos in discrete nonlinear dynamical systems, *Chaos Soliton. Fract.*, **18** (2003), 775–783. https://doi.org/10.1016/S0960-0779(03)00028-6

43. R. Ahmed, M. Rafaqat, I. Siddique, M. A. Arefin, Complex dynamics and chaos control of a discrete-time predator-prey model, *Discrete Dyn. Nat. Soc.*, **2023** (2023), 8873611. https://doi.org/10.1155/2023/8873611

44. G. P. Jiang, W. X. Zheng, A simple method of chaos control for a class of chaotic discrete-time systems, *Chaos Soliton. Fract.*, **23** (2005), 843–849. https://doi.org/10.1016/j.chaos.2004.05.025

AIMS Press